Energy Conversion and Management 186 (2019) 156–167

Contents lists available at ScienceDirect

Energy Conversion and Management

journal homepage: www.elsevier.com/locate/enconman

Dual intake rotary vane expander technology: Experimental and theoretical assessment

Fabio Fatigati*, Marco Di Bartolomeo, Roberto Cipollone

University of L'Aquila, Department of Industrial and Information Engineering and Economics, Via Giovanni Gronchi n.18, 67100 L'Aquila, Italy

ARTICLE INFO

Keywords:
Dual intake port expanders
Waste heat recovery
ORC
Rotary vane expanders

ABSTRACT

Rotary Vane Expander is an interesting solution for small-scale ORC power unit due to its reliability, flexibility and competitive cost. As demonstrated by the authors in previous works, the introduction of a secondary intake port leads to an increase of the aspirated mass flow rate and consequently of the mechanical power produced by the machine. In this paper, theoretical and experimental studies were conducted in order to assess the potential benefits in terms of efficiency introduced by the dual intake expander and the trade-off with the produced power for a given pressure-drop. The theoretical results showed that if the relative gain of mechanical power produced by the dual intake technology is higher than that of working fluid mass flow rate, the efficiency grows when the same machines operate at the same upstream and downstream pressures. Two expanders have been designated, built and tested giving the possibility to experimentally verify the performances of a single and a double intake machine. From measured data a mathematical model of the expander was validated, allowing to use it as a virtual platform for further machine optimization and improvement. It was observed that the efficiency gain introduced by the dual intake device depends on the OEM volumetric efficiency and on the pressure ratio. The global efficiency of the dual intake expander grows up to 30% if the volumetric efficiency is 50% and the pressure ratio is 2.3 while the efficiency benefit decreases to 5% if the volumetric efficiency is 70% and the pressure ratio is 3. Nevertheless, even if the global efficiency would be equal for the two machines, the dual intake technology always allows to increase the delivered mechanical power.

1. Introduction

In the last two decades the main effort of the researchers in the transport sector has been addressed towards the reduction of the ICE polluting emissions, bounded by restrictive international regulations. In particular, strict limitations have been introduced to reduce CO_2 emissions in order to counteract the climate change. UE by 2020 sets a target of 95 g CO_2/km and 147 g CO_2/km for average emissions of passenger cars and light commercial vehicles respectively [1,2]. Therefore, the most important challenge that scientific community will have to face is the decrease of fuel consumption as well as the energy demand on board maintaining at the same time high performances of ICEs if not increasing them. More recently, energy recovery became an important challenge because the efficiency of modern ICEs does not exceed 40%, [3], and the remaining energy from the fuel is wasted to the environment, mainly on the exhaust gases and coolant, [4]. Waste heat recovery technologies allow to reuse the waste heat of ICE converting it into mechanical or electric energy ensuring the improvement in performance and emissions of the engine, [5]. Among the waste heat recovery technologies Organic Rankine Cycle could be a promising solution [4,6]. ORC power units are quite conventional for large applications while there are still some critical issues in smaller scale applications, in particular in the transportation sector, [7]. Main limiting factors are the weight increase of the vehicle, the engine back pressure caused by the evaporator, the condenser frontal area occupation [7] and the time-varying temperature and flow rate of the thermal source which does not match with a recovery unit thought for steady applications.

Among the components of the ORC based power unit, the expander is certainly the less conventional device and its design for small scale applications is a technological challenge [8,9] especially when unconventional working fluids are used, [10]. The expander can be classified as dynamic or positive displacement type. The choice of the best technological solution should be performed taking into account the operating conditions, the efficiency and the cost without neglecting other engineering aspects (geometry, leakages, heat dissipation etc.), [11].

Turbo-expander should be adopted when rotational speeds and

* Corresponding author.
E-mail address: fabio.fatigati@univaq.it (F. Fatigati).

https://doi.org/10.1016/j.enconman.2019.02.026
Received 3 October 2018; Accepted 9 February 2019
Available online 01 March 2019
0196-8904/

Nomenclature

Symbols

A	area [m^2]
$A_{clearance}$	clearance area [m^2]
d	equivalent diameter [m]
h	working fluid specific enthalpy [J/kg]
L	length of the port [m]
L_{leak}	length of leakage flow [m]
m	working fluid mass [kg]
$\dot{m}$	working fluid mass flow rate [kg/s]
N_v	number of the vanes
n	expander revolution speed [rad/s], [RPM]
P	power [W]
p	pressure [Pa], [bar]
Q	volumetric flow rate [m^3/s]
T	temperature [K], [°C]
U_{wall}	relative velocity between blades and stator [m/s]
V	volume [m^3]

Greek symbols

$\Delta\dot{m}$	working fluid mass flow rate increase [%]
ΔP	Power increase [%]
Δp	pressure difference [Pa], [bar]
$\Delta\theta$	angular extent [rad], [deg]
$\Delta\eta$	global efficiency increase [%]
δ	minimum clearance [m]
η	expander global efficiency [%]
η_v	expander volumetric efficiency [%]
θ	angular position [rad], [deg]
μ	dynamic viscosity [Pa·s]
ρ	working fluid density [kg/m^3]
$\Phi_{dual\ int}$	dual intake port circumferential position [rad], [deg]

Subscripts

blade	blade
covers	gap between rotor and covers of the casing
dual int	dual intake port expander
dual int, end	dual intake port closing angle
dual int, start	dual intake port opening angle
exh, end	exhaust port closing angle
exh, start	exhaust port opening angle
ind	indicated power
is, exhaust	specific enthalpy at exhaust in isentropic condition
mech	mechanical power
mech, lost	mechanical power lost due to friction
main int, end	main intake port closing angle
main int, start	main intake port opening angle
out	outlet
side	gap between blade side and rotor
tip	gap between blade tip and stator
vane	vane
WF	working fluid

Acronyms

EM	Electric Motor
Evap	Evaporator
FF	Filling Factor
OEM	Original Equipment Manufacturing
PHX cond	Plate Heat Exchanger condenser

power are high, [12]. Considering real working conditions, radial machines should be preferred with respect to the axial one due its low flexibility and mechanical to electric conversion efficiency, [8]. Alshammari et al. [12] developed and experimentally characterized a Waste Heat Recovery System (WHRS) in a heavy duty diesel engine. A radial inflow turbine was designed for the specific application and its performance as well as the overall cycle one were assessed. The results showed that at 40% engine load the maximum generated power was 6.3 kW and the peak efficiency of the turbine was 35.2% at 20000 rpm while the maximum thermal efficiency of the cycle was 4.3%. Guillaume et al. [13] performed an experimental campaign of an ORC system with a radial-inflow turbine comparing the performances of two different working fluids, R245fa and R1233zd. The maximum electric power was 3.5 kW and the overall efficiency of the turbine, averaged on all experimental cases, was about 28%. Bahadormanesh et al. [14] developed a design procedure for radial turbines using different working fluids performing an optimization algorithm based on firefly method for ORC application. As objective function, the ORC thermal efficiency and the radial turbine size parameter were chosen while the constraints were vibration and stress. The study shows that the constraints have a significant effect on the optimum decision variable and the size of the turbine decreases as the shaft speed grows. Moreover, the exploration of Pareto front showed that with a little decrease in the efficiency of the turbine it is possible to achieve a great reduction of its size. In higher power applications, Kang [15] developed design and experimental procedures to assess the performance of an ORC with a two stage radial turbine using R245fa as working fluid. The results showed that maximum electric power and mean cycle and turbine efficiencies were 39 kW, 9.8% and 58.4% respectively. Tesla turbine, which is a viscous bladeless device, could be an interesting alternative for small-micro power generation, [16]. Talluri et al. [16] carried out a design procedure of a Tesla turbine for ORC applications introducing an innovative rotor model and performed an optimization method in order to evaluate the losses of each component. Manfrida et al. [17] elaborated a revised Tesla turbine design and they observed an efficiency up to 50% with azeotropic mixtures.

Volumetric machines are suitable for small scale applications due to their low rotational speed, low flow rate for high pressure ratios and their acceptance of two-phase flows, [18]. There are different typologies of volumetric expanders (screw, piston, scroll, sliding vane, swash plate) and a large set of parameters such as the cycle operating conditions, the system compactness, the components availability and the cost determine which is the best technology.

Dumont et al. [19] compared 4 different volumetric expanders: screw, scroll, piston and roots type using R245fa as working fluid. They observed that the efficiency is 76% for scroll, 53% for screw and piston and 48% for roots. Ziviani et al. [20] performed a theoretical comparison between single screw and scroll expander. They found that single screw expander allows to achieve a higher ORC overall efficiency with respect to scroll machine. A huge literature is available on the expander's choice which, for the sake of simplicity, here it is neglected having limited the references to the last 4 years.

Sliding vane expanders had a lower interest in literature recently revamped by the authors. They involve minor costs being characterized by a simpler geometry with respect to scroll and screw expanders and present the typical disadvantages of volumetric devices: internal leakages, friction, need of lubrication, [21]. Kolasiński et al. [22] carried out an experimental investigation on a domestic CHP ORC system using a multi-vane expander and R123 as working fluid. The results revealed a maximum internal efficiency of 58.3% due to vane leakages, pressure fluctuations in supply and discharge and vortexes. In particular, main leakages were found to exist between vane tips and stator and from

supply to exhaust ports. The study reported in [23] suggested that the increase of the vanes number can reduce this phenomenon at the expense, however, of higher friction losses.

Bianchi et al. [24] through a validated CFD model of a sliding vane expander observed that leakages influence the indicated diagram. Vodicka et al. [25] through a semi-empirical model demonstrated that the leakages significantly affect the isentropic efficiency and the filling factor. Masush et al. [26] built different test rigs with volumetric expander and MM as working fluid. Nominal power for the different test rigs varied from 1 to 10 kW. Isentropic efficiencies varied from 25% to 58% while the filling factor ranged from 1 to 6 for the bigger machine with a built-in volume ratio of 8. The results showed that internal leakages played an important role not allowing the system to reach the design maximum pressure. Cipollone et al. [27] developed an ORC application coupled with a heavy duty diesel internal combustion engine using R236fa as working fluid. Sliding vanes technology has been used both for the expander and for the pump. Net power output ranges from 0.7 kW to 2 kW for different ESC-13 operating points of the ICE reaching an expander overall efficiency of about 50%.

The limiting factors presented by volumetric machines are thus represented by low mechanical and indicated efficiency and limited power due to lower allowable revolution speed with respect to the dynamic ones. In order to overcome these limiting factors the authors developed a novel technology based on the introduction of an auxiliary intake port (dual intake). From a conceptual point of view, keeping the same upstream and downstream pressure, the dual intake expander allows an increase of the mass flow rate and, consequently, of the power. Mechanical efficiency is expected to remain constant because it is mainly due to inertial effects rather than pressure difference across the vanes. On the other hand, indicated efficiency can grow considering that it is a ratio between two different quantities both increasing with the dual intake port technology. Following an equivalent analysis, for the same mass flow rate a similar delivered power can be expected with a lower upstream pressure. In [28] a sensitivity analysis on the angular position and the diameter of an auxiliary suction port was conducted to realize a dual intake device in order to increase the output power of the machine. The study showed that, once optimized these parameters, a power output increase in the order of 50% is possible.

In the present work a numerical and experimental characterization of the dual intake expander was performed demonstrating the consistency of the theoretical expectations. Two different machines (single and dual intake port) were designed, built and tested. The measured data from the different experimental campaigns were subsequently used to validate a numerical model which was used as a virtual platform to further investigate the characteristics and performances of the two different devices comparing them at constant upstream and downstream pressure. Through the installation of three piezo-resistive sensors the indicated cycles were assessed in both cases in order to compare them with the calculation of the indicated power. Moreover, an analytic study was done in order to analyze the potential benefits in terms of global efficiency achieved with the dual intake port expander. Through the comparison of the dual intake port expander and OEM models, a parametric analysis was conducted to determine the effects on the global efficiency increase of geometric parameters such as the circumferential position of the secondary port, its angular extent and area. Finally, the comparison between the supercharged machine and the OEM was developed varying the pressure ratio for different volumetric efficiency of the machine.

2. Experimental characterization of the expander

In order to experimentally characterize the expander, an ORC power unit was developed and fully instrumented. The working fluid adopted is R236fa in order to compare the expander performances with the results of previous experimental activities performed by the authors [27,28]. The higher thermal source is represented by the exhaust gases of a IVECO F1C a 3L, supercharged, diesel engine while the cold one is tap water. The ORC is composed by the following components:

- Pump: A gear pump driven by an asynchronous electric motor which circulates and pressurizes the working fluid. Thanks to an inverter the revolution speed of the pump can be varied so the working fluid mass flow rate circulating in the plant is a control parameter;
- Evaporator: The working fluid outgoing from the pump flows and vaporizes in a plate and fin heat exchanger specifically designed to reduce the backpressure effects on the ICE;
- Expander: A rotary vane expander with radial suction and axial exhaust port in which the working fluid coming from the evaporator can expand. The mechanical to electric power conversion is obtained by an asynchronous generator connected to the electric network. For this reason the expander is forced to rotate at around 1500 RPM;
- Condenser: A plate heat exchanger cooled by tap water in which the working fluid was condensed. Subsequently, it flows in a tank located upstream the pump in order to dump the pulsation of the mass flow rate.

In Fig. 1 a scheme of the experimental layout is reported. As can be observed pressures and temperatures of the working fluid were measured upstream and downstream each component. The working fluid mass flow rate was measured through a Coriolis flowmeter while the cooling water mass flow rate by a magnetic one.

Torque and revolution speed were measured on the shaft of the expander and of the pump. In order to better understand the behavior of the expander, the pressure inside the vanes during the shaft rotation was measured through the introduction of three piezo-resistive sensors suitably placed on the expander's casing and sequenced in time. Therefore, the indicated cycle can be assessed thus evaluating the mechanical efficiency as the ratio between the shaft power and the indicated power. Knowing the pressure inside the vane and assuming an isothermal suction phase (hypothesis sustained by CFD analyses) it is possible to define the density at the inlet port closing. This quantity ensures to assess the volumetric efficiency η_v of the expander according to Eq. (1):

$$\eta_v = \frac{N_v \rho V_{end,intake} n}{\dot{m}_{WF,in}} \tag{1}$$

where:

N_v is the number of the vanes;
ρ is the working fluid density at end of the intake phase;

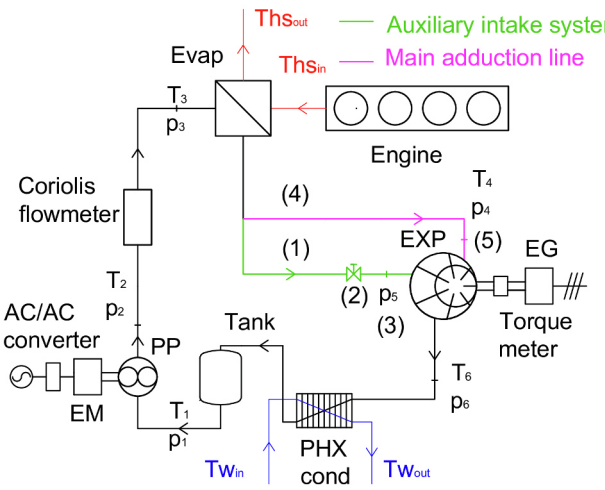

Fig. 1. Scheme of the ORC Power Unit test bench.

$V_{end,intake}$ the vane volume at end of the intake phase;
n is the expander revolution speed;
$\dot{m}_{WF,in}$ is the mass flow rate at the expander inlet.

The volumetric efficiency η_v is evaluated as the reciprocal of the filling factor currently considered in literature and it shows that only a part of the $\dot{m}_{WF,in}$ is introduced inside the expander. In fact, the difference between the mass of the working fluid measured downstream the pump and that inside the vane at the end of the intake phase (evaluated through Eq. (1)) is due to the volumetric losses (i.e. the fluid that escapes through the cover of the expanders and the blades).

The position of the pressure transducers reported in Fig. 2 allows the evaluation of a part of the whole indicated cycle of the machine. The remaining one was completed through the numerical model of the expander developed by the authors. Considering the accuracy of the pressure transducers, the uncertainties related to the evaluation of the indicated cycle are in the order of 2% according to the approach reported in [29].

Once the expander has been experimentally characterized, the auxiliary intake port was introduced on the machine, adopting the circumferential position defined in [28] which approaches the condition of maximum mechanical power increase. The position of the auxiliary port is represented as the difference between the auxiliary (dual) intake port opening angle and the main intake port closing angle (Fig. 2). The angular extent and the area of the auxiliary port are reported in Table 1. The introduction of the dual intake system involves a slight modification of the ORC test bench. In particular, two different pipes downstream the evaporator feed the expander through the main and the auxiliary intake ports. An additional Coriolis mass flow-meter has been introduced in order to measure the two mass flow rates in addition to a regulation valve which allows to control the mass flow rate feeding the auxiliary port. This new arrangement increases the permeability of the machine, i.e. the ratio between the mass flow rate provided by the expander and the pressure difference (upstream and downstream the machine). Keeping the same expander upstream and downstream pressure, the overall flow rate increases. Furthermore, for the same produced mass flow rate, the upstream pressure decreases.

3. Theoretical model of the expander

The theoretical model of the expander was developed in GT-Suite™ environment following the approach used in [28,30]. The model reproduces, following a 1-D transient approach, the filling and emptying processes occurring in the intake and exhaust pipes while a lumped parameter model describes the evolution of pressure and temperature inside the vanes. In both cases, mass, momentum and energy conservation equations are solved. The fluid-dynamic of the working fluid is described through the resolution of the Navier-Stokes equations which represent the mass, momentum and energy conservation.

The aforementioned conservation laws are solved in the following way:

- Intake and exhaust are discretized with a 1-D approach in space;
- Two static pressures are fixed at the beginning of the intake and at the end of the exhaust pipe;
- The internal elements are calculated with respect to the conservation laws of mass, momentum and energy allowing the evaluation of friction losses and concentrated pressure drops (inflow/outflow, deviations etc.);
- The knowledge of the passage section towards the vane allows to represent the mass flow rate entering the vane as well as the coexistence of multiple vanes fillings. According to this, pressure inside the vanes changes in time. Similarly the auxiliary intake and the emptying of the vanes is treated;
- When the vane is a closed volume the model follows a lumped representation according to an adiabatic isentropic transformation;
- The mass inside the vanes changes due to flow leakages occurring across them (tip leakages);
- The model accounts for 2 main important leakages: flow across the vanes and flow across the covers. The first one is the main contribution and it is modelled through the Poiseuille/Couette relation for flow between parallel plates according to Eq. (2):

$$Q = A_{clearance}\left(\frac{\Delta_{tip}{}^2\Delta p}{12\mu L_{leak}} + \frac{1}{2}U_{wall}\right) \quad (2)$$

In Eq. (2) $A_{clearance}$ is the clearance area, Q is the volume flow rate, δ_{tip} is the minimum clearance between blade tip and inner stator surface, Δp is the pressure difference, μ is the dynamic viscosity, L_{leak} is the length of leakage flow and U_{wall} is the relative velocity between moving and fixed components. As δ is hardly measurable it is set through a calibration procedure in order to minimize the difference between the predicted and experimental mass flow rate values. Eq. (2) describes also the leakage between blade side and rotor slot (the corresponding minimum clearance is δ_{side}), nevertheless, this volumetric loss is negligible with respect to that at blade tip.

The other leakages are modelled through an equivalent orifice whose diameter d_{covers} is chosen so that its area is equal to the leakage gap surface across the covers, [31];

- An iterative procedure is needed in order to match the thermo-fluid-dynamics inside the intake and the exhaust pipes and the relevant data inside the vanes. Reconstructing the p-V values the indicated power can be evaluated;
- Regarding the mechanical power 3 major losses are considered:
  1. Friction losses at blade tip;
  2. Friction losses on the blade side;
  3. Viscous losses on the end-wall plates.

The first 2 contributions depend on the normal reactions (with respect to the relative speed) and on an equivalent friction coefficient. The former quantity derives from the equilibrium of the forces (Newton laws) while the latter from tuning the predicted overall friction losses and the difference between indicated and measured mechanical power. The third contribution depends upon the axial clearance between rotor and stator;

- Having the fluid a real behavior, an equation of state is included according to NIST™ database.

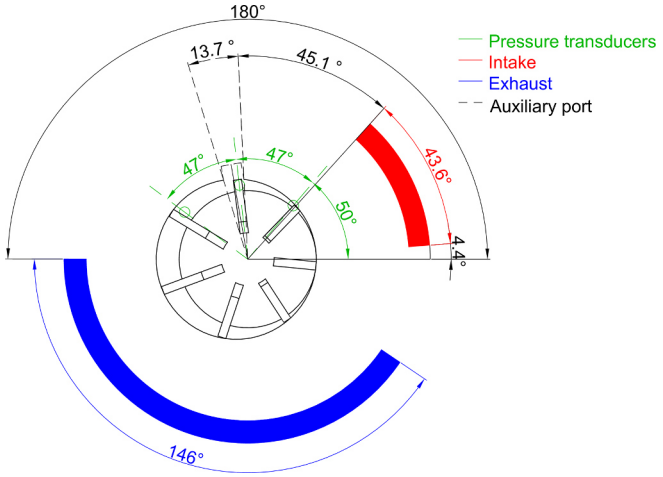

Fig. 2. Configuration of suction and exhaust port and the piezo-resistive sensors position.

Table 1
Configuration of auxiliary intake port.

Auxiliary intake port configuration	
Circumferential position	45.1°
Area	72.3 (mm^2)
Angular extent	13.7°

4. Experimental validation of the OEM and dual intake expander models

The model has been validated on the data collected during the experimental activity. As previously noted three steps of validation have been considered:

- The predicted mass flow rate provided by the pump and that actually introduced inside the vane are compared with the corresponding experimental values. If the errors are low the model allows to correctly represent the volumetric losses. In fact, only a part of the mass flow rate sent by the pump enters the expander, the remaining one flows across the tip blade or across the covers;
- A further validation is done through the comparison between predicted and measured indicated cycle. So this comparison behaves like a guarantee for the whole procedure;
- Once the indicated power is calculated the measured shaft power gives the possibility to evaluate the friction losses suffered by the machine.

The OEM model has been validated through the data reported in Table 2 collected after a wide experimental campaign. The intake pressure p_{in} varies between 8.5 bar and 10.6 bar while the pressure imposed by the circuit at the expander outlet p_{out} and inlet temperature T_{in} were comprised in a range of 4.1 bar to 4.8 bar and 74.5 °C and 90.7 °C respectively. The revolution speed is fixed to 1500 rpm as the expander is connected to the electric network via an asynchronous generator while the maximum produced mechanical power is 647 W and the minimum one is 447 W.

In Table 3 the relative percentage errors between the predicted and experimental values of the validation quantities have been reported. Maximum percentage deviations are 5% for indicated and mechanical power and 6.7% and 9.3% for mass flow rate and volumetric efficiency respectively. As can be observed the model allows to accurately represent the real behavior of the expander. This aspect is also demonstrated by the good agreement between the experimental and numerical indicated cycle (pV diagram) as reported in Fig. 3. The figure shows how the numerical indicated cycle describes with a good accuracy the experimental one. In particular, the model allows the description of the not isobaric suction of the device, which can be due to volumetric losses or to the increase of vane volume during intake phase.

Concerning the expansion phase, both numerical and experimental pressure trends show a deviation from the theoretical adiabatic trend with no leakages. The different trend is due to the clearances between vane tips and stator. The effects of leakages on indicated cycle is well known in literature, [23,24].

Table 3
Relative Percentage Error between numerical and experimental data.

	1	2	3	4	5	6	7	8
$\dot{m}_{WF}$	4.6%	4.2%	1.3%	1.3%	1.2%	6.7%	2.2%	2.9%
P_{ind}	0.4%	3.0%	−2.4%	0.3%	−5.1%	0.5%	−4.2%	−5.0%
P_{mec}	2.5%	0.2%	−0.1%	5.0%	2.8%	2.5%	1.0%	2.7%
η_v	2.2%	2.7%	6.0%	9.3%	7.2%	−0.4%	5.4%	4.9%

During the calibration of the model, it was found that there are only a set of constructive gaps (Table 4) which ensure to minimize the error between the predicted and experimental values of the mass flow rate provided by the pump and of the indicated power. This means that the model is able to reproduce the mass inside the vane during the rotation because it determines the pressure in the chamber.

The low value of η_v can be due to the not optimal lubrication condition of the machine, as the oil ensures to increase the sealing across the leakage path. Therefore, in order to improve the performance of the expander, a deep analysis on the behavior of the lubrication oil in the machine will be necessary.

The model of the dual intake expander has been validated on the experimental data reported in Table 5. The validation was conducted with the same approach followed for the OEM expander. The only difference is that for the dual intake machine the model should be able to predict also the mass flow rate flowing into the expander via the auxiliary intake port.

The validation phase demonstrated that the model allows to reproduce with good accuracy the real behavior of the dual intake port expander. Percentage relative errors with respect to the experimental data for the main parameter of interest are reported in Table 6. Maximum deviations are 7.2%, −4.6% and 4.3% for total mass flow rate, auxiliary mass flow rate and indicated power respectively.

In Fig. 4 the experimental pV diagram of the dual intake expander and the comparison with the one predicted by the model have been reported. It can be noticed that, when the dual intake port opens, the pressure raises after a decrease in the last part of main intake phase. The auxiliary port was located in order to feed the expander as soon as the main intake port was closed. Thus, the pressure was kept constant through the intake of further mass of working fluid until the dual intake ends whereupon the pressure decrease due to the expansion. Generally, the pressure inside the vane at the outlet port opening is higher than that imposed by the circuit downstream the expander so a quasi-isochoric expansion takes place.

5. Theoretical analysis of the effects of the dual intake port on the expander global efficiency

A theoretical analysis has been conducted to evaluate the

Table 2
Experimental data of operating condition and expander performance.

Case	1	2	3	4	5	6	7	8
p_{in} ± 0.3 [bar_a]	8,5	8,9	9,5	10,2	10,6	8,2	9,3	10,1
p_{out} ± 0.3 [bar_a]	4.1	4.3	4.5	4.7	4.8	4.0	4.3	4.6
T_{in} ± 0.3 [°C]	74.5	79.4	78.6	80.2	83.6	77.9	81.5	90.7
T_{out} ± 0.3 [°C]	54.0	59.9	61.9	64.3	67.5	59.4	63.4	72.1
n ± 1 [RPM]	1524.5	1527.3	1529.1	1533.0	1535.2	1524.0	1528.5	1532.9
P_{ind} ± 2% [W]	540	560	640	690	777	513	657	738
P_{mec} ± 0.8% [W]	471	513	559	593	647	447	560	616
$\dot{m}_{WF}$ ± 0.15% [kg/s]	0.095	0.100	0.110	0.118	0.122	0.089	0.105	0.112
η_v [%]	48	48	47	46	47	49	47	47
η_{OEM} [%]	43	43	42	41	42	43	42	42

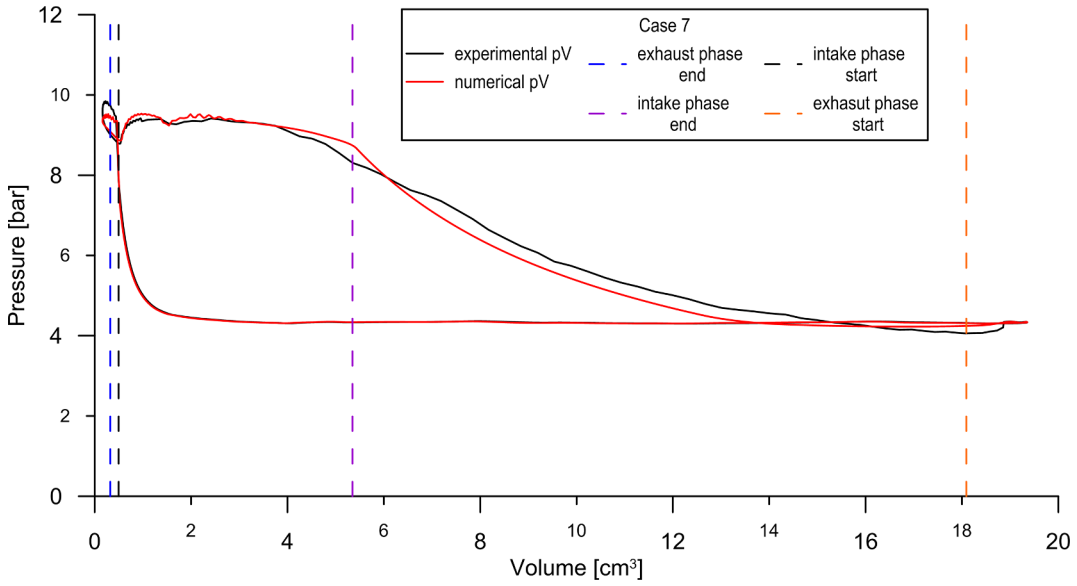

Fig. 3. Experimental and numerical pV diagram for case 7.

Table 4
Clearances of the constructive gap resulting from the calibration of the model.

Clearance δ between vane tip and stator	δ_{tip} = 85 μm
Clearance δ between vane side and rotor slot	δ_{side} = 5 μm
Clearance between rotor and casing (equivalent diameter)	d_{covers} = 0.2 mm
Friction factor	0.1

improvements on global efficiency related to the introduction of an auxiliary intake port. For the sake of simplicity, the global efficiency of the expander η_{OEM} was evaluate in Eq. (3) as the ratio between mechanical power P_{mech} and isentropic power; this is strictly valid if an isentropic expansion takes place till to the downstream pressure of the plant. A more correct expression should consider the isochoric expansion which happens when the exhaust port opens leading the fluid to the pressure at the condenser.

$$\eta_{OEM} = \frac{P_{mech}}{\dot{m}_{WF}(h_{intake} - h_{is,exhaust})} = \frac{P_{ind} - P_{mech,lost}}{\dot{m}_{WF}(h_{intake} - h_{is,exhaust})} \quad (3)$$

Having expressed the mechanical power as the difference between indicated (P_{ind}) and mechanical power lost ($P_{mech,lost}$) due to dry and viscous friction, the expression of the global efficiency for the dual intake port case $\eta_{dual\ int}$ can be written as in Eq. (4):

$$\eta_{dual\ \ int} = \frac{(P_{ind} + \Delta P_{ind}) - (P_{mech,lost} + \Delta P_{mech,lost})}{(\dot{m}_{WF} + \Delta\dot{m}_{WF})(h_{intake} - h_{is,exhaust})} \quad (4)$$

where:

– ΔP_{ind} represents the difference between the indicated power P_{ind} of the dual intake port expander and the OEM;
– $\Delta P_{mech,lost}$ is the difference between the mechanical power lost $P_{mech,lost}$ of the dual intake port expander and the OEM;
– $\Delta\dot{m}_{wf}$ is the difference between the working fluid mass flow rate $\dot{m}_{WF}$ provided by the dual intake port expander and the OEM.

Table 6
Relative Percentage Error between numerical and experimental data for dual intake port expander.

	9	10	11	12	13	14	15
$\dot{m}_{wf,main}$	−3.2%	5.4%	7.2%	1.6%	−0.8%	−1.4%	−3.8%
$\dot{m}_{wf,dual\ int}$	1.5%	−4.6%	−3.9%	1.9%	0.2%	0.1%	1.6%
P_{ind}	−3.2%	−0.4%	2.3%	3.6%	4.3%	−1.0%	4.3%

The difference between the global efficiencies of the two machines ($\eta_{dual\ int}$ and η_{OEM}) is therefore (Eq. (5)):

$$\Delta\eta = \frac{(P_{ind} + \Delta P_{ind}) - (P_{mech,lost} + \Delta P_{mech,lost})}{(\dot{m}_{WF} + \Delta\dot{m}_{WF})(h_{intake} - h_{is,exhaust})} - \frac{P_{ind} - P_{mech,lost}}{\dot{m}_{WF}(h_{intake} - h_{is,exhaust})} \quad (5)$$

Thus, the global efficiency of the expander with auxiliary intake port is greater than the OEM value if Eq. (6) is satisfied:

$$\Delta\eta > 0 \rightarrow \frac{\Delta P_{ind} - \Delta P_{mech,lost}}{P_{ind} - P_{mech,lost}} > \frac{\Delta\dot{m}_{WF}}{\dot{m}_{WF}} \quad (6)$$

which implies Eq. (7):

Table 5
Results of experimental characterization of dual intake port expander.

Case	9	10	11	12	13	14	15
p_{in} ± 0.3 [bar_a]	6.4	6.1	6.0	5.6	5.3	5.3	5.0
$p_{dual\ int}$ ± 0.3 [bar_a]	5.9	5.6	5.4	5.2	4.9	4.9	4.5
p_{out} ± 0.3 [bar_a]	3.6	3.6	3.1	3.3	3.1	3.1	3.1
T_{in} ± 0.3 [°C]	79.5	78.9	77.2	70.4	77.2	77.4	76.7
T_{out} ± 0.3 [°C]	71.9	72.8	69.5	63.3	71.2	71.6	72.9
n ± 1 [RPM]	1517.8	1516.6	1521.8	1513.8	1512.3	1513.0	1510.5
P_{ind} ± 2% [W]	528	502	623	475	439	444	357
$\dot{m}_{wf,main}$ ± 0.15% [kg/s]	0.061	0.049	0.050	0.047	0.044	0.044	0.041
$\dot{m}_{wf,dual\ int}$ ± 0.15% [kg/s]	0.070	0.080	0.081	0.073	0.067	0.066	0.059

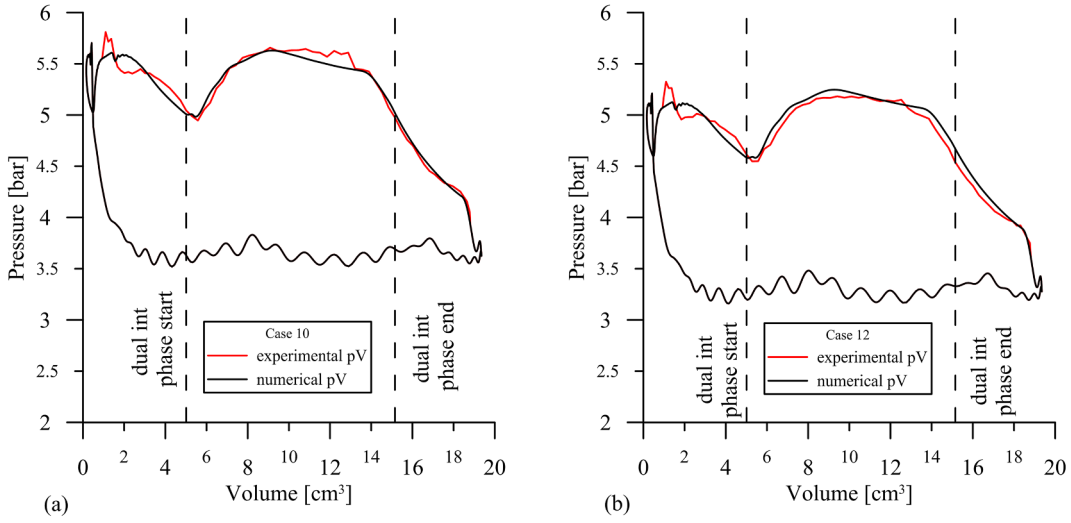

Fig. 4. Comparison between experimental and numerical pV diagram for case 10 and for case 12.

$$\Delta\eta > 0 \rightarrow \frac{\Delta P_{mech}}{P_{mech}} > \frac{\Delta \dot{m}_{WF}}{\dot{m}_{WF}} \tag{7}$$

Eq. (7) demonstrates that the expander with the dual intake port ensures a greater global efficiency if the relative percentage increase of mechanical power is higher than that of the mass flow rate in the OEM case. Therefore, if the condition expressed in Eq. (7) is satisfied, the dual intake port technology is not only a way to recover more power increasing the mass flow rate but it also ensures to improve the global efficiency of the expander.

6. Comparison between dual intake port expander and OEM

The global efficiency of the dual intake port expander was evaluated varying the configuration of the auxiliary intake port in terms of its circumferential position $\Phi_{dual\ int}$, its area $A_{dual\ int}$ and the angular extent $\Delta\theta_{dual\ int}$. The circumferential position $\Phi_{dual\ int}$ (Fig. 5) is expressed as the difference between the dual intake port opening angle $\theta_{dual\ int,start}$ and the main intake port closing angle $\theta_{main\ int,end}$ (i.e. $\Phi_{dual\ int}$ is equal to zero when the auxiliary suction port is an extension of the main intake one while if $\Phi_{dual\ int} = -\Delta\theta_{dual\ int}$ the auxiliary intake port is contained inside the main intake one and this case is considered equal to the OEM). The area of the auxiliary suction port $A_{dual\ int}$ is represented by the diameter $d_{dual\ int}$ (Eq. (8)) of an equivalent circular section.

$$d_{dual\ \ int} = 2\sqrt{\frac{A_{dual\ \ int}}{\pi}} \tag{8}$$

where $A_{dual\ int}$ can be expressed as a function of the length of the port L and the angular extent of auxiliary intake port $\Delta\theta_{dual\ int}$. The configuration parameters of dual intake port can be observed in Fig. 5.

The comparison with the OEM was conducted varying the circumferential position of the auxiliary port $\Phi_{dual\ int}$ for different values of equivalent diameter $d_{dual\ int}$ and angular extent of the port $\Delta\theta_{dual\ int}$. The results of the comparison are expressed in terms of the variation of the global efficiency $\Delta\eta$, working fluid mass flow rate $\Delta\dot{m}_{wf}$ and produced mechanical power ΔP_{mech}.

Fig. 6 (a) and (b) are drawn for a fixed equivalent diameter $d_{dual\ int}$ equal to 7 mm and for an angular extent of the auxiliary port $\Delta\theta_{dual\ int}$ of 7° and 12.5° respectively. As can be observed, for both cases the dual intake port expander ensures a significant increase of global efficiency $\Delta\eta$ for a wide range of auxiliary port circumferential position $\Phi_{dual\ int}$. Moreover, increasing the angular extent of the auxiliary port $\Delta\theta_{dual\ int}$ the maximum $\Delta\eta$ is achieved for $\Phi_{dual\ int}$ equal to 30.4° for case (a) and 25.5° for case (b) which both lead the absolute value of the global efficiency $\eta_{dual\ int}$ to 53%. Indeed, as $\Delta\theta_{dual\ int}$ grows, the $\Phi_{dual\ int}$ which ensures the maximum increase of global efficiency $\Delta\eta$, decreases, approaching the position of auxiliary intake port to that of the main intake one. Fig. 6 (a) and (b) show that the dual intake port expander has a global efficiency higher than the OEM ($\Delta\eta_{gobal} > 0$) according to Eq. (7).

The benefit in terms of $\Delta\eta$ disappear ($\Delta\eta_{gobal} = 0$) for a circumferential position $\Phi_{dual\ int}$ equals to 73.8° for case (a) and 68.2° for case (b). In both cases the end of auxiliary intake phase coincides with the start of the exhaust one ($\theta = 151.3$). In fact, the intake phase ends when the vane no longer faces the corresponding port. According to the adopted reference system (Fig. 5), this happens when θ fulfills the condition expressed by the Eq. (9):

$$\theta = \theta_{main\ \ int,end} + \Phi_{dual\ \ int} + \frac{\Delta\theta_{vane}}{2} + \Delta\theta_{dual\ \ int} - \frac{\Delta\theta_{blade}}{2} \tag{9}$$

For higher $\Phi_{dual\ int}$, the dual intake phase and the exhaust phase overlap and a considerable amount of mass flow rate flows directly to the exhaust without exchanging work with the machine, thus worsening the expander performance. This aspect is demonstrated by the sharp increase of $\Delta\dot{m}_{wf}$ and by the decrease of ΔP_{mech}.

The analysis carried out for $d_{dual\ int}$ equals to 15 mm reported in Fig. 6 (c) and (d) confirmed the observed trends. In particular, the

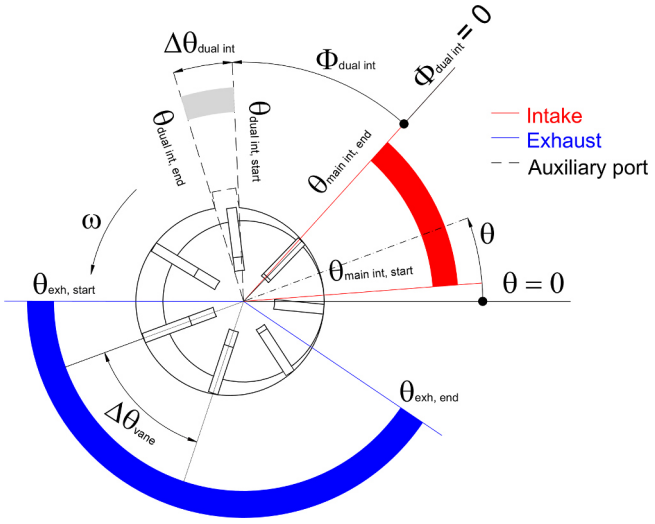

Fig. 5. Configuration of a dual intake port expander.

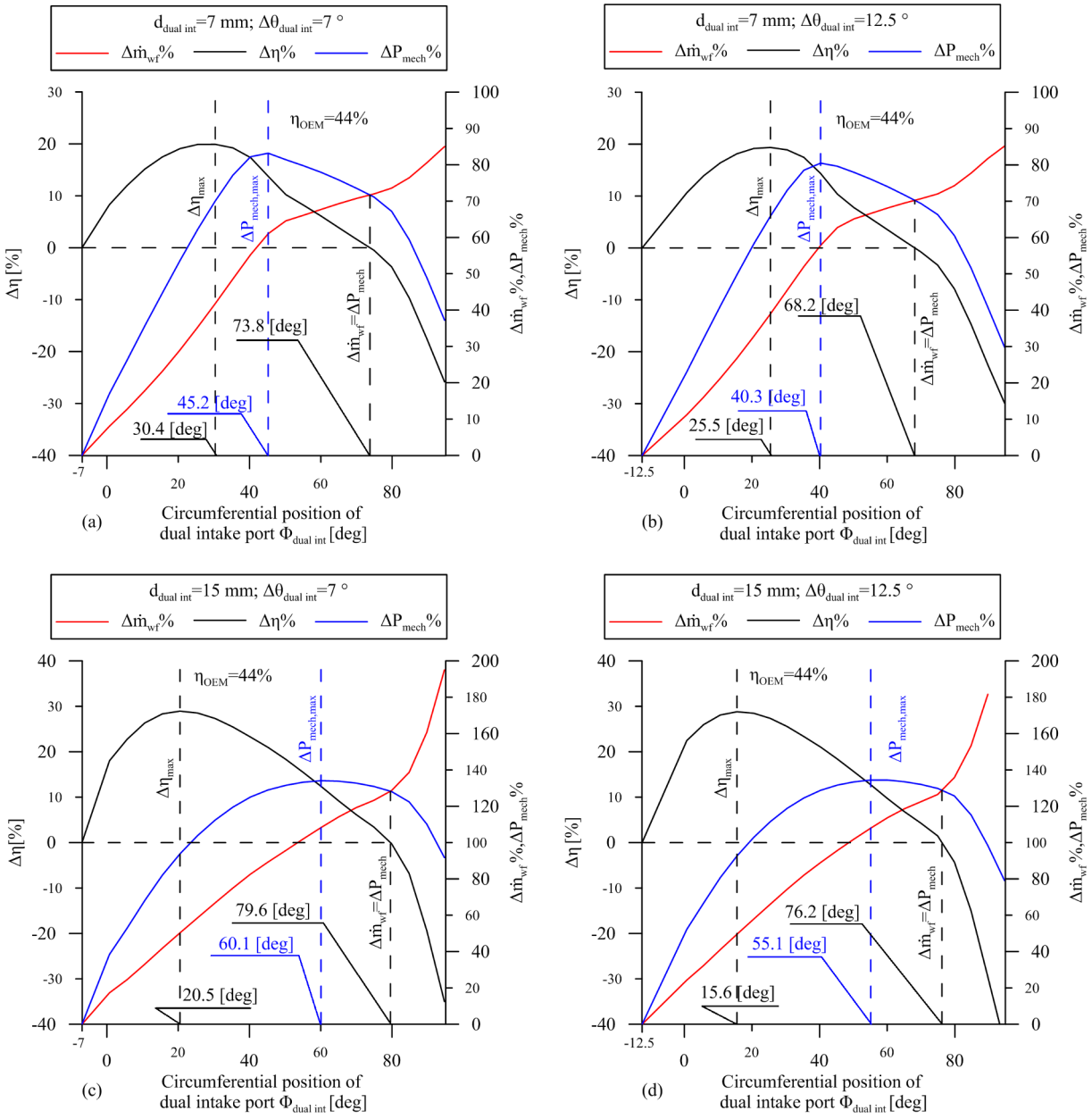

Fig. 6. Comparison between dual intake port expander and OEM varying $\Phi_{dual\ int}$ for different values of $d_{dual\ int}$ and $\Delta\theta_{dual\ int}$. (a) $d_{dual\ int}$ = 7 mm; $\Delta\theta_{dual\ int}$ = 7°; (b) $d_{dual\ int}$ = 7 mm; $\Delta\theta_{dual\ int}$ = 12.5°; (c) $d_{dual\ int}$ = 15 mm; $\Delta\theta_{dual\ int}$ = 7°; (d) $d_{dual\ int}$ = 15 mm; $\Delta\theta_{dual\ int}$ = 12.5°.

maximum $\Delta\eta$ is achieved for $\Phi_{dual\ int}$ equals to 20.5° and $\Phi_{dual\ int}$ equals to 15.6°, respectively, both leading to 57% absolute global efficiency. Therefore, for a fixed $\Delta\theta_{dual\ int}$, the circumferential position $\Phi_{dual\ int}$ which maximizes the global efficiency slightly changes increasing the d_{int}: adopting a higher d_{int}, the trend of $\Delta\eta_{global}$ is quite the same, simply increased of a scale factor.

Moreover, Fig. 6 shows that there is a range in which both the efficiency and mechanical power considerably increase regardless of the angular extent of the second port and of the equivalent diameter. Maximum global efficiency and mechanical power growths are in the order of 20–30% and 80–140% respectively. However, the circumferential angular position $\Phi_{dual\ int}$ corresponding to the maximum global efficiency does not ensure the maximum increase of mechanical power ΔP_{mech}. Maximum ΔP_{mech} is achieved with the dual intake port located in a circumferential position $\Phi_{dual\ int}$ which ensures that the dual intake phase starts few degrees after the end of the main intake one, as reported in [28]. On the other hand, the value of $\Phi_{dual\ int}$ to which corresponds the maximum $\Delta\eta$ involves that the main and auxiliary intake phases are partially overlapped.

In Fig. 7 (a), (b), (c) and (d) the comparison between the indicated cycle (pV diagram) of the dual intake expander and that of the OEM is reported. Moving from Fig. 7 (a) to (d), $\Phi_{dual\ int}$ increases. In case (a) the two ports are angularly adjacent (limiting case) while in (b), (c) and (d) the opening of the second port is progressively delayed. The last case, Fig. 7 (d), represents the situation where the closing of the second intake port coincides with the opening of the discharge one. Moving from (a) to (d), the dual intake phase happens for higher vane volumes so the pressure at discharge port opening increases. This causes a stronger isochoric expansion and severe oscillations during the discharge phase. Nevertheless, the corresponding indicated power values P_{ind} (reported on the figures) show that the maximum is obtained in Fig. 7 (d) when the mass flow rate elaborated by the machine is higher with respect to other cases. In fact, P_{ind} grows with the mass flow rate aspirated by the expander until the dual intake phase is not overlapped

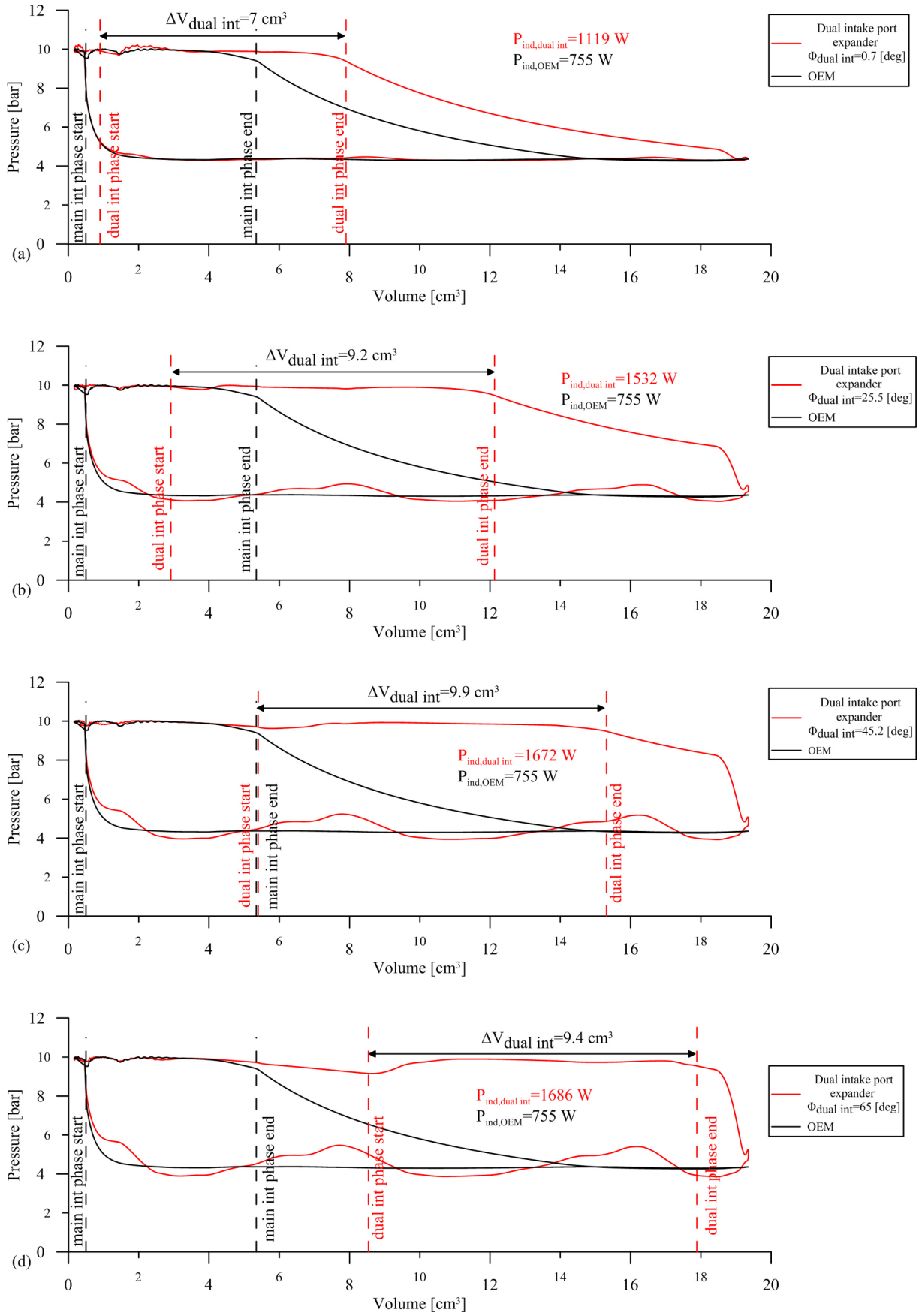

Fig. 7. Comparison between the indicated cycle (pV diagram) of dual intake and OEM expander varying $\Phi_{dual\ int}$: (a) $\Phi_{dual\ int}$ = 0.7 [deg]; (b) $\Phi_{dual\ int}$ = 25.5 [deg]; (c) $\Phi_{dual\ int}$ = 45.2 [deg]; (d) $\Phi_{dual\ int}$ = 65 [deg].

Table 7
Theoretical case with volumetric efficiency of 70% (Case A) and 85% (Case B).

	OEM ref	OEM Case A	OEM Case B
η_v [%]	47	70	85
η_{global} [%]	44	55	62
p_{in} [bar]	10	10	10
p_{out} [bar]	4.3	4.3	4.3
T_{in} [°C]	80.7	80.7	80.7
Clearance between blade tip and stator δ_{tip} [μm]	85	40	20
Clearance between blade side and rotor slot δ_{blade} [μm]	5	5	5
Clearance between rotor and covers (equivalent diameter) d_{covers} [mm]	0.2	0.2	0.2

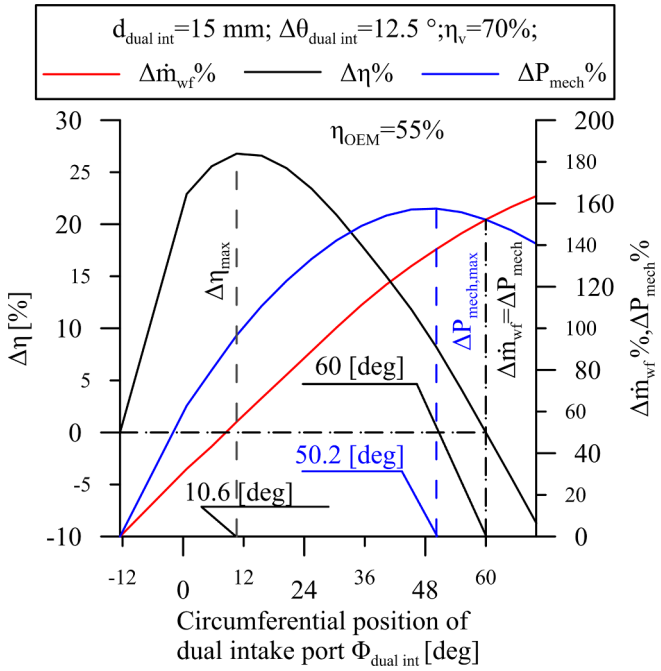

Fig. 8. Case A- Comparison between dual intake port expander and OEM (η_v = 70%) varying $\Phi_{dual\ int}$ for $d_{dual\ int}$ = 15 mm and $\Delta\theta_{dual\ int}$ = 12.5°.

with the discharge one. Therefore, if $\Phi_{dual\ int}$ is higher than in case (d), the indicated power decreases due to the overlapping of the dual intake and of the discharge phases. Anyway, the dual intake expander shows the capability to elaborate a greater mass flow rate with respect to the OEM. This aspect leads to a higher flexibility which can be particularly important for applications in which the thermal power available at the hot source can easily exceeds the design conditions (as it happens in the transportation sector).

7. Effects of OEM volumetric efficiency and upstream pressure on benefits introduced by dual intake port technology

Even though the obtained value (and used) for η_v is in a strict agreement with the present literature, a so low value invites to extend the analysis of the dual intake technology to a more refined (and precious) machine in which the η_v would be higher. Therefore, in order to assess in a wider way the potential benefits of the dual intake port expander, the analysis was repeated considering two theoretical cases where the OEM expander has a η_v of 70% and 85% respectively. In order to perform this prediction, the constructive clearances between vane tip and stator, (while other constructive gaps were kept constant) have been reduced in the models until the η_v values were reached. The

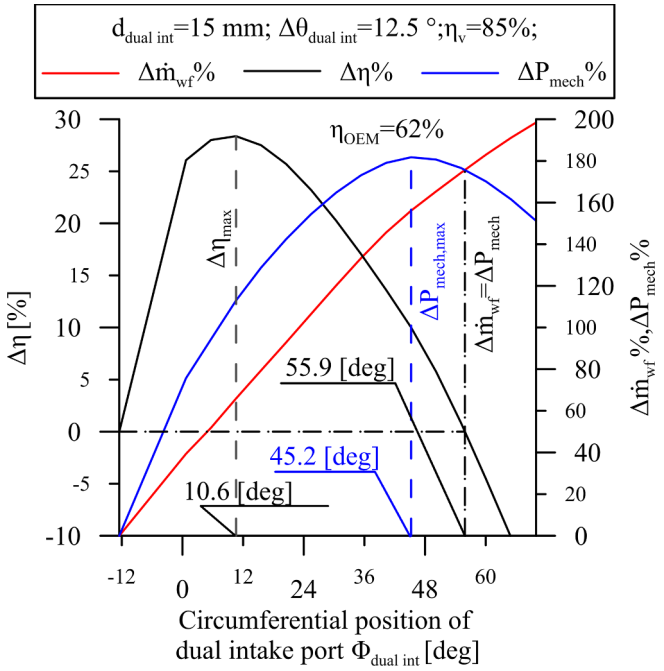

Fig. 9. Case B- Comparison between dual intake port expander and OEM (η_v = 85%) varying $\Phi_{dual\ int}$ for $d_{dual\ int}$ = 15 mm and $\Delta\theta_{dual\ int}$ = 12.5°.

considered operating conditions and the dimensions of the clearances are reported in Table 7 as predicted by the mathematical model of the expander. Table 7 reports also the data (OEM ref) referred to the tested expander.

Fig. 8 shows the results of the global efficiency increase $\Delta\eta$ and other relevant quantities for Case A in Table 7. The dual intake technology ensures $\Delta\eta$ similar to that obtained for a less refined machine (Fig. 6): maximum $\Delta\eta$ is close to 27%. Being the global efficiency of the OEM reference case equal to 55% (assuming the better η_v value), an absolute value of the new global efficiency ranks at 70%.

A difference with respect to the OEM reference case is the narrower range of circumferential positions $\Phi_{dual\ int}$ which guarantees η greater than the OEM case. This is due to the position of the dual intake port which ensures the fulfilment of Eq. (7) so the value of $\Phi_{dual\ int}$ where this happens diminishes. When $\Phi_{dual\ int}$ decreases, the opening of the auxiliary intake port gets closer to the end of the main intake one: in the case of Fig. 8, the maximum global efficiency increase is reached few degrees after the main intake port closing angle ($\Phi_{dual\ int}$ = 10.6°). Moreover, in this condition an increase of the mechanical power close to 97% is reached due to the higher aspirated mass flow rate ($\Delta\dot{m}_{wf}$ = 55%). Another interesting result is obtained for a circumferential position which ensures the same global efficiency of the single intake expander. In Fig. 8 this happens when $\Phi_{dual\ int}$ is equal to 60°: in this case, a power increase of 150% is obtained. Wide ranges of $\Phi_{dual\ int}$ with greater mechanical power but lower global efficiency with respect to OEM are evident. For instance, at $\Phi_{dual\ int}$ = 65°, a 4.3% reduction of the global efficiency guarantees a 147% increase of the produced mechanical power. Fig. 9 shows the performances of Case B reported in Table 7. Similar global efficiency increases are reachable with a slightly narrower range of $\Phi_{dual\ int}$ with respect to case A. Figs. 8 and 9 show that the global efficiency increase due to the introduction of dual intake port still happens for more refined machines (see data in Table 7) even though the ranges of $\Phi_{dual\ int}$ tend to reduce.

Data reported in Table 7 could justify an increase in the friction power (mechanical efficiency decrease due to the clearance reduction till to 20 μm) but if the machines are properly designed this would not happen: the oil film which is pressurized by the blade tip contact and which sustains the blade itself in equilibrium is self-pressurized as it

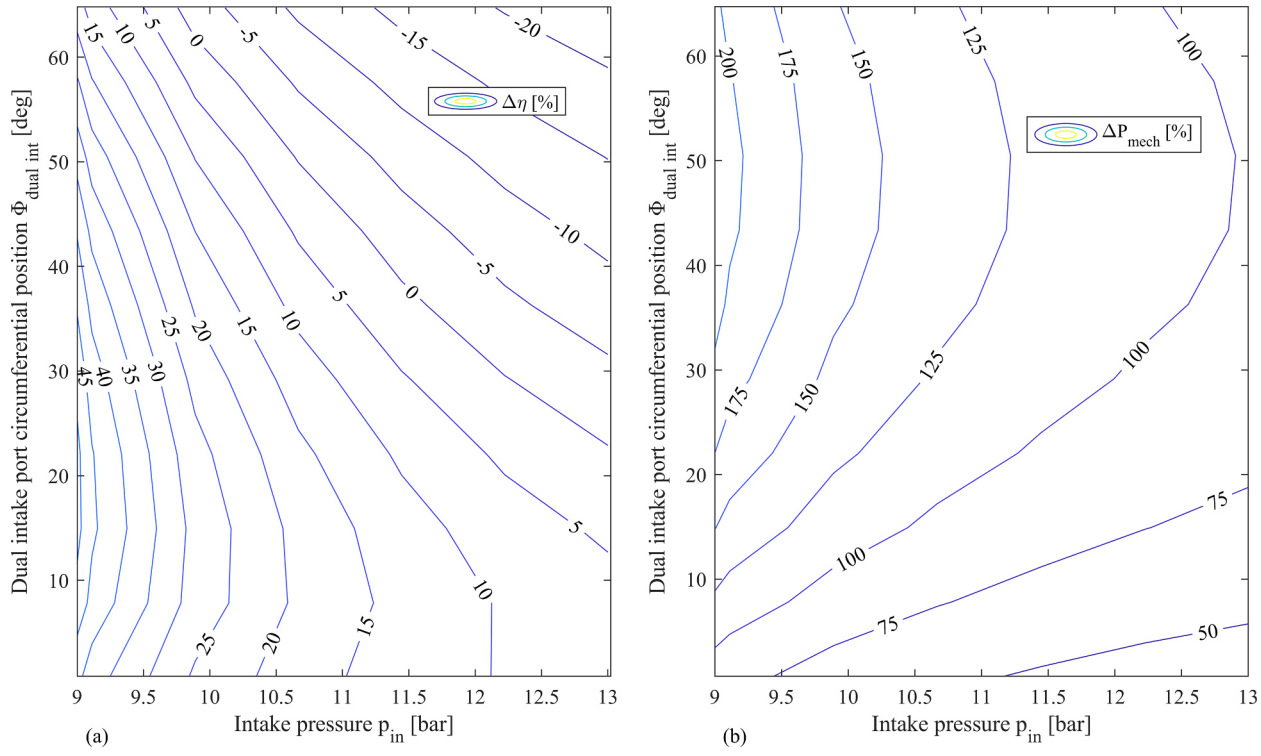

Fig. 10. Case A-(a) Global efficiency Δη and (b) mechanical power ΔP_{mech} gain (%) achieved with dual intake technology with respect OEM varying the intake pressure and dual intake port circumferential position $\Phi_{dual\ int}$ for a fixed discharge pressure (4.3 bar).

happens in the case of an hydrodynamical bearing, [32].

In Fig. 10 (a) the effect of the variation of the intake pressure (keeping constant the pressure imposed by the circuit at the expander outlet) on Δη achieved with the dual intake port technology is reported for case A. In ORC-based power units, intake pressure p_{in} is determined by the mass flow rate provided by the pump and also by the amount of thermal power exchanged at the evaporator. These variations are significant considering those of the engine operating conditions. This fact negatively affects the performance of the expander with a single intake because of: (a) improper vane filling, (b) mismatch between the pressure variations produced by the built-in-volume ratio inside the machine and the upstream and downstream pressure ratio of the machine itself (imposed by the system).

Fig. 10 (a) demonstrates that the dual intake port technology produces a benefit, increasing the operating flexibility of the machine in terms of operating pressures. Indeed, the dual intake expander ensures global efficiency gain Δη up to 45% for lower p_{in} (with respect to a value at the design point), for the whole range of $\Phi_{dual\ int}$ considered. On the other hand, as p_{in} grows the range of $\Phi_{dual\ int}$ shrinks and Δη decreases. Fig. 10 (b) reports the effects on the mechanical power (or indicated power considering that the friction power doesn't change significantly). The percentage values ΔP_{mech} are higher when p_{in} decreases but significant positive variations are present also for larger p_{in} ranging from 50% to 100%, depending on the circumferential position of dual intake port $\Phi_{dual\ int}$. Therefore, although for a specific p_{in} the benefits of the dual intake are not guaranteed ($\Delta\eta_{global} = 0$) being possible lower efficiencies with respect to the single intake ($\Delta\eta_{global} < 0$), the increase in produced mechanical power is always significant (ΔP_{mech} = 100–125%).

Therefore, the dual intake port technology extends the operating flexibility of the device and allows to keep the global efficiency close to the design value also when the machine operates in off-design conditions. Indeed, the global efficiency of the dual intake port expander is always higher than that of the OEM except for higher intake pressure p_{in} and circumferential position $\Phi_{dual\ int}$ of the auxiliary intake port far from the main one. Nevertheless, also in this condition the dual intake port expander ensures to increase the produced mechanical power up to 125% allowing to recover more energy from the exhaust gases thus compensating the expander percentage global efficiency decrease.

8. Conclusions

Rotary vane expanders represent a suitable solution for small scale ORC power unit, nevertheless, they still have some limiting aspects. The main concern is due to the flow leakages through the clearance between blade tip and stator and across the covers. These volumetric losses lead to a reduction of the volumetric efficiency making the performances of the expander worse. A further critical aspect is represented by friction power resulting from the mechanical interaction between the blades and the stator. This paper was referred to the improvement of the sliding vane rotary expander and discusses a novel technology which improved both volumetric and mechanical efficiency. A conventional sliding vane rotary expander (OEM) was modified considering an auxiliary intake port circumferentially sequenced with respect to the main one, the new machine is so called dual intake port expander. Theoretical and experimental activities were performed to demonstrates the improvements achievable with the introduction of dual intake port. Its design has been done through a comprehensive mathematical model of the machine once it was experimentally validated. In order to validate the mathematical model, the OEM expander has been tested in a wide range of operating conditions being part of an ORC-based power unit. Main relevant machine properties were measured including the p-V diagram thanks to a sequence of piezo-resistive transducers angularly spaced. After the design phase, the dual intake expander prototype was built and tested. In all the tested cases, the software platform predicted in a very precise way the experimental evidences allowing to justify the increased performances produced by the new technology and allowing a deep understanding of the involved phenomena. Volumetric and mechanical efficiencies were determined and, consequently, an optimization of the position of the second intake

port was produced.

For a fixed upstream pressure, the following conclusions and design considerations apply:

- For machines with low η_v (high filling factor), the dual intake port technology allows a great potential of improvement. The analysis shows a wide range of circumferential positions of the second intake with a considerable increase of the machine global efficiency up to 30%: this is the result of the indicated power increase. The dual intake port always allows an increase of the working fluid mass flow rate and consequently of the produced mechanical power till a maximum of 140%;
- For more refined machines the dual intake port still improves the performances. If the initial volumetric efficiency and mechanical efficiency are higher (volumetric efficiency of machine even more refined ranking respectively 70% and 85%), the maximum global efficiency improvement is comprised between 27% and 28 % with a mechanical power increase close to 100%;
- The auxiliary intake port technology doesn't change significantly the power lost by friction; main contribution to the friction power is produced by tip blade interaction with the stator while the side friction (machine covers) is almost negligible;
- The dual intake port technology increases the permeability of the machine seen from the plant side; this allows to decrease, for a given mass flow rate, the upstream pressure of the expander with positive benefits for the overall plant behavior. For a given upstream pressure, the more permeable machine produces a working fluid flow rate increase which allows an additional machine flexibility due to the possibility of increasing the thermal recovery at the higher temperature source.

Declaration of interests

The authors declare that they have no known competing financial interests or personal relationships that could have appeared to influence the work reported in this paper.

Acknowledgment

The authors are grateful to Ing. Enea Mattei S.p.A, its CEO, Dr. Giulio Contaldi, and Dr. Stefano Murgia for the support during this research activity.

References

[1] REGULATION (EC) No 443/2009 OF THE EUROPEAN PARLIAMENT AND OF THE COUNCIL of 23 April 2009, setting emission performance standards for new passenger cars as part of the Community's integrated approach to reduce CO_2 emissions from light-duty vehicles.
[2] REGULATIONS REGULATION (EU) No 510/2011 OF THE EUROPEAN PARLIAMENT AND OF THE COUNCIL of 11 May 2011 setting emission performance standards for new light commercial vehicles as part of the Union's integrated approach to reduce CO_2 emissions from light-duty vehicles.
[3] Pischinger R, Klell M, Sams T. Thermodynamik der Verbrennungskraftmaschine. 3rd ed. New York: Springer; 2010.
[4] Horst Tilmann Abbe, Tegethoff Wilhelm, Eilts Peter, Koehler Juergen. Prediction of dynamic Rankine Cycle waste heat recovery performance and fuel saving potential in passenger car applications considering interactions with vehicles' energy management. Energy Convers Manage 2014;78:438–51. ISSN 0196-8904.
[5] Saidur R, Rezaei M, Muzammil WK, Hassan MH, Paria S, Hasanuzzaman M. Technologies to recover exhaust heat from internal combustion engines. Renew Sustain Energy Rev 2012;16(8):5649–59. https://doi.org/10.1016/j.rser.2012.05.018. ISSN 1364-0321.
[6] Jiménez-Arreola Manuel, Pili Roberto, Wieland Christoph, Romagnoli Alessandro. Analysis and comparison of dynamic behavior of heat exchangers for direct evaporation in ORC waste heat recovery applications from fluctuating sources. Appl Energy 2018;216:724–40. https://doi.org/10.1016/j.apenergy.2018.01.085. ISSN 0306-2619.
[7] Di Battista Davide, Di Bartolomeo Marco, Villante Carlo, Cipollone Roberto. On the limiting factors of the waste heat recovery via ORC-based power units for on-the-road transportation sector. Energy Convers Manage 2018;155:68–77. https://doi.org/10.1016/j.enconman.2017.10.091. ISSN 0196-8904.
[8] Cipollone R, Di Battista D, Bettoja F. Performances of an ORC power unit for waste heat recovery on heavy duty engine. Energy Procedia 2017;129:770–7. https://doi.org/10.1016/j.egypro.2017.09.132. ISSN 1876-6102.
[9] Fiaschi Daniele, Innocenti Gianmaria, Manfrida Giampaolo, Maraschiello Francesco. Design of micro radial turboexpanders for ORC power cycles: From 0D to 3D. Appl Therm Eng 2016;99:402–10. https://doi.org/10.1016/j.applthermaleng.2015.11.087.
[10] Macchi E, Perdichizzi A. Efficiency prediction for axial-flow turbines operating with unconventional fluids –transactions of the ASME. J Eng Power 1981;103:719.
[11] Ziviani Davide, Beyene Asfaw, Venturini Mauro. Advances and challenges in ORC systems modeling for low grade thermal energy recovery. Appl Energy 2014;121:79–95. https://doi.org/10.1016/j.apenergy.2014.01.074. ISSN 0306-2619.
[12] Alshammari Fuhaid, Pesyridis Apostolos, Karvountzis-Kontakiotis Apostolos, Franchetti Ben, Pesmazoglou Yagos. Experimental study of a small scale organic Rankine cycle waste heat recovery system for a heavy duty diesel engine with focus on the radial inflow turbine expander performance. Appl Energy 2018;215:543–55. https://doi.org/10.1016/j.apenergy.2018.01.049. ISSN 0306-2619.
[13] Guillaume Ludovic, Legros Arnaud, Desideri Adriano, Lemort Vincent. Performance of a radial-inflow turbine integrated in an ORC system and designed for a WHR on truck application: an experimental comparison between R245fa and R1233zd. Appl Energy 2017;186(Part 3):408–22. https://doi.org/10.1016/j.apenergy.2016.03.012. ISSN 0306-2619.
[14] Bahadormanesh Nikrouz, Rahat Shayan, Yarali Milad. Constrained multi-objective optimization of radial expanders in organic Rankine cycles by firefly algorithm. Energy Convers Manage 2017;148:1179–93. https://doi.org/10.1016/j.enconman.2017.06.070. ISSN 0196-8904.
[15] Seok Hun Kang. Design and preliminary tests of ORC (organic Rankine cycle) with two-stage radial turbine. Energy 2016;96:142–54. https://doi.org/10.1016/j.energy.2015.09.040. ISSN 0360-442.
[16] Talluri L, Fiaschi D, Neri G, Ciappi L. Design and optimization of a Tesla turbine for ORC applications. Appl Energy 2018;226:300–19. https://doi.org/10.1016/j.apenergy.2018.05.057. ISSN 0306-2619.
[17] Manfrida G, Pacini L, Talluri L. An upgraded Tesla turbine concept for ORC applications. Energy 2018;158:33–40. https://doi.org/10.1016/j.energy.2018.05.181. ISSN 0360-5442.
[18] Galindo J, Ruiz S, Dolz V, Royo-Pascual L, Haller R, Nicolas B, et al. Experimental and thermodynamic analysis of a bottoming Organic Rankine Cycle (ORC) of gasoline engine using swash-plate expander. Energy Convers Manage 2015;103:519–32. https://doi.org/10.1016/j.enconman.2015.06.085. ISSN 0196-8904.
[19] Dumont Olivier, Parthoens Antoine, Dickes Rémi, Lemort Vincent. Experimental investigation and optimal performance assessment of four volumetric expanders (scroll, screw, piston and roots) tested in a small-scale organic Rankine cycle system. Energy 2018. https://doi.org/10.1016/j.energy.2018.06.182. ISSN 0360-5442.
[20] Ziviani D, Suman A, Lecompte S, De Paepe M, van den Broek M, Spina PR, et al. Comparison of a single-screw and a scroll expander under part-load conditions for low-grade heat recovery ORC. Syst Energy Procedia 2014;61:117–20. https://doi.org/10.1016/j.egypro.2014.11.920. ISSN 1876-6102.
[21] Kolasiński P. The Influence of the heat source temperature on the multivane expander output power in an Organic Rankine Cycle (ORC) system. Energies 2015;8:3351–69.
[22] Kolasiński Piotr, Błasiak Przemysław, Rak Józef. Experimental investigation on multi-vane expander operating conditions in domestic CHP ORC system. Energy Procedia 2017;129:323–30. https://doi.org/10.1016/j.egypro.2017.09.201. ISSN 1876-6102.
[23] Kolasiński P, Błasiak P, Rak J. Experimental and numerical analyses on the rotary vane expander operating conditions in a micro organic Rankine cycle system. Energies 2016;9:606.
[24] Bianchi Giuseppe, Rane Sham, Kovacevic Ahmed, Cipollone Roberto, Murgia Stefano, Contaldi Giulio. Numerical CFD simulations on a small-scale ORC expander using a customized grid generation methodology. Energy Procedia 2017;129:843–50. https://doi.org/10.1016/j.egypro.2017.09.199. ISSN 1876-6102.
[25] Vodicka Vaclav, Novotny Vaclav, Mascuch Jakub, Kolovratnik Michal. Impact of major leakages on characteristics of a rotary vane expander for ORC. Energy Procedia 2017;129:387–94. https://doi.org/10.1016/j.egypro.2017.09.249. ISSN 1876-6102.
[26] Mascuch Jakub, Novotny Vaclav, Vodicka Vaclav, Zeleny Zbynek. Towards development of 1–10 kW pilot ORC units operating with hexamethyldisiloxane and using rotary vane expander. Energy Procedia 2017;129:826–33. https://doi.org/10.1016/j.egypro.2017.09.196. ISSN 1876-6102.
[27] Cipollone Roberto, Bianchi Giuseppe, Gualtieri Angelo, Di Battista Davide, Mauriello Marco, Fatigati Fabio. Development of an Organic Rankine Cycle system for exhaust energy recovery in internal combustion engines. J Phys Conf Ser 2015;655(1):012015.
[28] Fatigati Fabio, Bianchi Giuseppe, Cipollone Roberto. Development and numerical modelling of a supercharging technique for positive displacement expanders. Appl Therm Eng 2018;140:208–16. https://doi.org/10.1016/j.applthermaleng.2018.05.046. ISSN 1359-4311.
[29] Bianchi Giuseppe, Cipollone Roberto. Theoretical modeling and experimental investigations for the improvement of the mechanical efficiency in sliding vane rotary compressors. Appl Energy 2015;142:95–107. https://doi.org/10.1016/j.apenergy.2014.12.055. ISSN 0306-2619.
[30] Fatigati Fabio. Exhaust gases waste heat recovery in ICEs: theoretical and experimental characterization of innovative technologies and plant solutions. PhD thesis; 2017.
[31] GT-Suite™ Flow Manual, General flow components. Gamma Technologies.
[32] Cipollone Roberto. Sliding vane rotary compressor technology and energy saving. Proc Inst Mech Eng E: J Process Mech Eng 2016;230(3):208–34. https://doi.org/10.1177/0954408914546146.

Gli autori dichiarano di aver contribuito in misura paritetica allo sviluppo del presente articolo scientifico: "Dual intake rotary vane expander technology: Experimental and theoretical assessment", pubblicato sulla rivista internazionale Energy Conversion and Management, (https://doi.org/10.1016/j.enconman.2019.02.026),

Gli Autori:

Fabio Fatigati

L'AQUILA, 24/09/2021

Marco Di Bartolomeo

L'AQUILA, 24/09/2021

Roberto Cipollone

L'AQUILA 24/09/2021